BENEFITS OF IMPROVED RESOLUTION FOR EDXRF

R. Redus[1], T. Pantazis[1], J. Pantazis[1], A. Huber[1], B. Cross[2]

[1]Amptek, Inc., 14 DeAngelo Dr, Bedford MA 01730, 781-275-2242, www.amptek.com
[2]CrossRoads Scientific, 414 Av. Portola, P.O. Box 1823, El Granada, CA 94018-1823

This is an extended version of a paper which was presented at the 2008 Denver X-Ray Conference and which has been submitted to "Advances in X-Ray Analysis".

Abstract

The accuracy and precision of energy dispersive X-ray fluorescence (EDXRF) improve with improved detector energy resolution. However, there are always trade-offs between the highest energy resolution and the highest count rates, there are practical difficulties in achieving the very best energy resolution, and there are many system level issues beyond energy resolution alone. Energy resolution is commonly used to differentiate systems but the benefits of improved energy resolution, in accuracy and precision of the analytical results, are not always clear. In the results reported here, EDXRF analysis has been carried out on a set of reference materials as a function of energy resolution. Several different detectors were used, including Si-PIN diodes, silicon drift diodes (SDD), and CdTe detectors. Their operating parameters were adjusted to give a range of energy resolutions. At 5.9 keV, the resolution ranged from 139 eV to 325 eV for SDD and Si-PIN devices, and to 450 eV for CdTe. The source was a 40 kVp W anode X-ray tube used in a backscatter geometry and the spectra were analyzed using the XRF-FP software.

1. Introduction

It is well known that improving the energy resolution of the spectrometer leads to improved precision in the results of XRF analysis but improved energy resolution nearly always comes with a penalty. Precision also depends on counting statistics and the highest energy resolution is obtained for small area detectors operated at long peaking times, implying relatively few counts. Detectors which combine the largest area and highest energy resolution are very expensive. Maximum cooling of the detectors can improve resolution for large areas, but this adds to system complexity and has a particularly large impact in portable systems. The designer of an EDXRF system is faced with the question: Which detector and operating conditions will maximize the precision and accuracy of the analytical result? How much benefit is gained from improving the energy resolution? The question was stated by Statham [1] as "Would a device that offered an excellent resolution of only 7 eV but could only acquire at 60 cps be more useful than a device that could acquire at 10,000 cps but gave much poorer performance of 150 eV?"

Statham examined this question theoretically for a few simple cases. Assuming that counting statistics alone determine random uncertainty in photopeak area, after subtracting background and overlapping photopeaks, he derived scaling rules for simple cases. In this paper, we compare these scaling rules to measured results with typical samples and also demonstrate how accuracy depends on energy resolution. In the first section of this paper, we briefly review Statham's results. In the remaining sections, we present experimental results showing how the precision and accuracy of the analytical results depends on the energy resolution of the spectrometer. Much of the data were obtained for stainless steel alloys, since "the analytical problems of stainless steel are typical for X-ray fluorescent spectrochemical analysis [2]". Results from other samples illustrate other important situations. Amptek's silicon drift diode

(XR100-SDD) was used to measure most of the spectra, since by controlling the temperature of the Peltier cooler, energy resolution can be varied while all other parameters are unchanged.

Precision quantifies the reproducibility of a result, which is the variation arising from random errors. It is observed in repeated measurements under identical conditions. Accuracy quantifies the correctness of a result, which arises from systematic errors. It is observed as the difference between the mean value of measurements and the true value [3]. This paper is concerned with the precision and accuracy of the reported concentration of the elements after the spectrum has been processed and corrected for matrix effects. The precision was measured as the standard deviation from many analyses (up to 400) of the same sample under the same conditions. The accuracy was measured as the difference between the results of chemical analyses and the mean of the EDXRF analyses. The accuracy measurements used Standard Reference Materials (SRMs) from the National Institute of Standards and Technology (NIST). The results are compared to confidence intervals specified by NIST for the chemical analysis methods.

2. Theoretical Results

We define σ to be the precision of the analytical result, i.e. the standard deviation of the reported concentration. N represents photopeak counts, δE is the FWHM energy resolution of the spectrometer, and κ is a constant. The first and simplest case considered by Statham is a single, isolated peak (no overlap with other peaks) and negligible background counts. In this case,

$$\sigma = \kappa N^{-0.5} \qquad [1]$$

The result depends only on the total counts in the photopeak, independent of energy resolution. For this limiting case, improving energy resolution will not help at all. The second case is a single, isolated peak on a large background, photopeak counts << background counts.

$$\sigma = \kappa \left(\delta E\right)^{0.5} N^{-0.5} \qquad [2]$$

Improving energy resolution reduces background counts, reducing the statistical uncertainty in background counts. For the next cases, precision scales as δE to an exponent n,

$$\sigma = \kappa \left(\delta E\right)^{n} N^{-0.5} \qquad [3]$$

where n depends on the details of the spectrum. The third case is two overlapping peaks, separated by much less than the energy resolution and of comparable intensity. For negligible background, the precision is proportional to the energy resolution, n=1. For strongly overlapping peaks on a large background, n=1.5. Additional overlap peaks increase n. For example, five overlapping peaks on a large background yield n=4.5. Statham's general conclusions are that reducing δE becomes increasingly important as (1) peaks get closer together, (2) peaks get smaller compared to the background or to tails of nearby peaks, and (3) the number of peaks to be deconvolved increases.

Consider how the precision improves with improved resolution. For the "low resolution" case, improving the resolution slightly improves precision dramatically, $\sim\delta E^{4.5}$. As δE improves, the peaks become separated and peak to background increases, so one obtains progressively less benefit from continued δE improvements. Eventually, in the "high resolution" limit the peaks are separated, background is negligible, and further reductions in δE have no benefit.

These results are simple and intuitive but leave a few key questions. Given the complexities of real world systems and samples, can one observe these scaling rules? These rules assume that

the only source of random variance is counting statistics, so is this a valid assumption? In a specific system and sample, at what energy resolution does the exponent change so that further improvements in δE are not beneficial? Since real spectra are likely to contain both isolated and overlapping peaks, how does one determine the overall optimum? Further, these results only apply to precision. How does the accuracy depend on energy resolution?

3. Experiment Description

The spectra were taken using Amptek's XR100 detectors. Most of the data used a silicon drift diode (SDD) with 6 mm^2 active area and 450 μm fully depleted thickness. A 6 mm^2 x 500 μm Si-PIN and a 25 mm^2 x 0.75 mm CdTe diode were used for some measurements [4, 5]. The detectors are mounted on a two-stage Peltier cooler in vacuum, which can achieve a temperature differential of 70K. They are behind a 1 mil Be window, with an internal collimator to restrict incident X-rays to the active volume for the Si diodes. Amptek's PX4 digital pulse processor provides trapezoidal pulse shaping with a wide range of time constants, an 8k channel MCA, and the functions of a conventional spectroscopy amplifier (pile-up rejection, dead time correction, etc.). The PX4 also includes the power supply, providing bias voltage and powering the Peltier cooler. At full cooling (220K under lab conditions) and at the noise corner (τ_p of 25.6 μsec), the SDD resolution was 139 eV FWHM at the 5.9 keV peak of Mn (electronic noise of 73 eV FWHM or 8.7 e^- rms). To vary the resolution while keeping all other parameters constant, the temperature set point of the Peltier cooler was raised. This increases leakage current, increasing shot noise and hence electronic noise but nothing else. For the SDD, the resolution ranged from 145 to 325 eV FWHM at the 5.9 keV K_α peak of Mn at τ_p of 9.6 μsec.

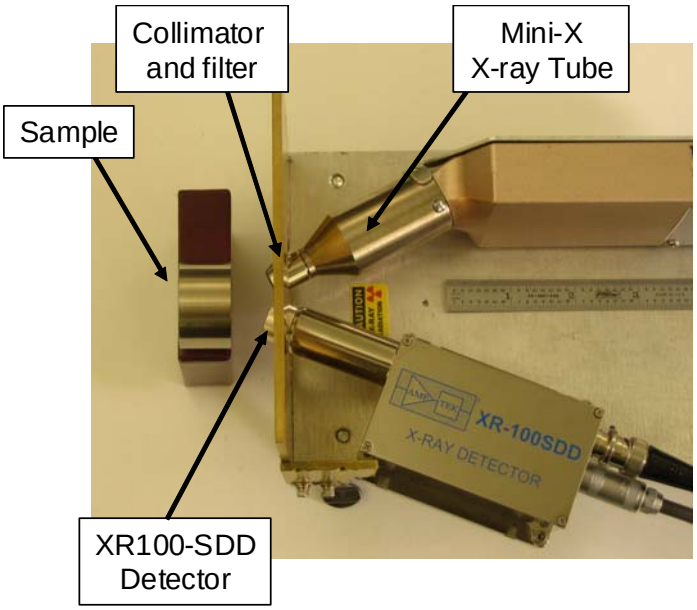

Figure 2. Photograph of the experimental spectrometer, based on Amptek's XR100-SDD detector, PX4 signal processor, Mini-X X-ray tube, and XRS-FP analysis software. The radiation shielding and the sample mount have been removed for clarity.

The excitation source for most of the measurements was Amptek's Mini-X, a compact 40 kVp X-ray tube from Comet AG with Amptek's control module, using a USB interface. This setup used a W anode transmission target tube with a 500 μm Al filter and an external collimator defining an 8° cone. Most of the data were taken at 30 kVp and 15-30 μA, providing a 10%

dead time unless otherwise noted. Both incidence and take-off angles were 67.5°, with approximately 1.5 cm from the target to the detector and to the front of the collimator.

The tube was controlled using Amptek's Mini-X software via USB interface. Amptek's ADMCA software was used to control the PX4 and to acquire and store the spectra, also via USB. Spectra were processed using the XRS-FP software, developed by CrossRoads Scientific and available through Amptek, Inc. This software provides spectrum processing, including correction for escape peaks and sum peaks, background removal, and spectral deconvolution. Nonlinear deconvolution with Gaussian peak fitting was used. Compositional analysis used a fundamental parameters algorithm.

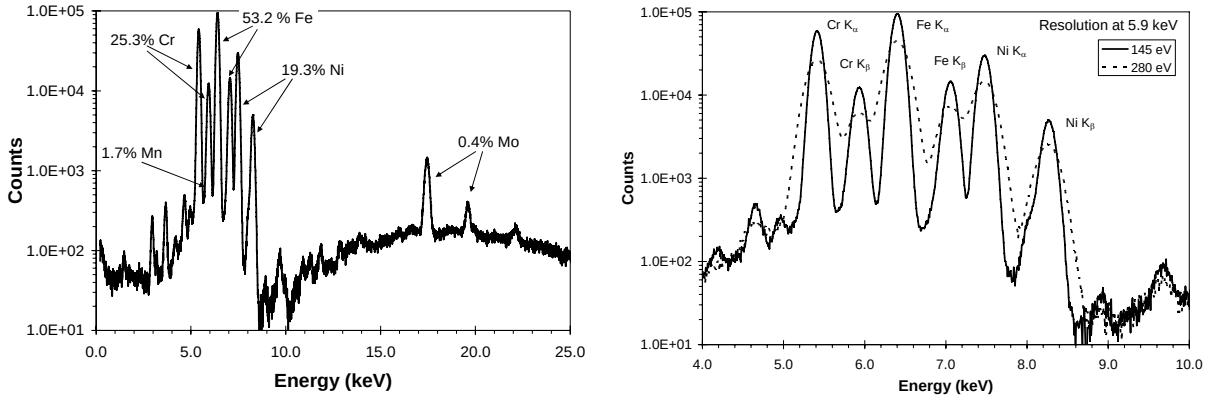

Figure 1. Plots showing the spectrum of stainless steel 310. Left: Full spectrum at full cooling, giving 145 eV FWHM at 5.9 keV. Right: Small portion of spectrum from 4 to 10 keV, at 145 eV FWHM (solid curve) and at 280 eV FWHM (dashed curve).

4. Experimental Results for Stainless Steel Alloys

Figure 1 shows 20 minute spectra at energy resolutions of 145 and 280 eV FWHM at 5.9 keV. The Fe, Ni, and Cr peaks are clearly visible. Cr is enhanced from the Fe and Ni X-rays produced in the sample, so these lines requires correction for matrix effects. These represent dominant peaks with some overlap and matrix correction. The Mo peaks are isolated from overlapping peaks, lying on a smooth background from brehmstrahlung, with photopeak area comparable to background. The Mn peaks are not visible in the raw data: the Mn K_α peak is at nearly the same energy as the Cr K_β, and the Mn K_β is at nearly the same energy as Fe K_α, with many more counts in the Cr and Fe peaks than Mn. The Mn peaks only appear through deconvolution, so represent the case of significant overlap and background.

Precision was measured using several stainless steel (SS) alloys. At each temperature (i.e. resolution), a 20 minute spectrum was obtained from a sample of SS 310. This single spectrum was used to calibrate FP. A sample of SS 347 was then placed in the apparatus and the software set in a "repetitive" mode to obtain 400, one minute spectra and automatically analyze each. The standard deviation of the 400 analysis results is the measured precision.

Figure 2 (left) shows the precision of the analysis result for Cr and Ni. The horizontal axis represents energy resolution at the Mn K_α peak, while the vertical axes show the precision (2σ) for Ni (left, solid) and Cr (right, dashed). The solid dots with error bars represent two standard deviations, computed from 400 measurements at each temperature. The open symbols represent a calculation of random uncertainty carried out in XRS-FP from photopeak area. The curves

represent a fit which assumes σ independent of δE at the lowest energies, then a $(\delta E)^{0.5}$ term at higher energies. These curves both match very well the results of Statham: the precision is independent of energy resolution below 200 eV, then scales as $(\delta E)^{0.5}$ above. For the curves, R^2 was 0.85 (0.91) for Cr (Ni). The computed uncertainty agrees with the observed uncertainty.

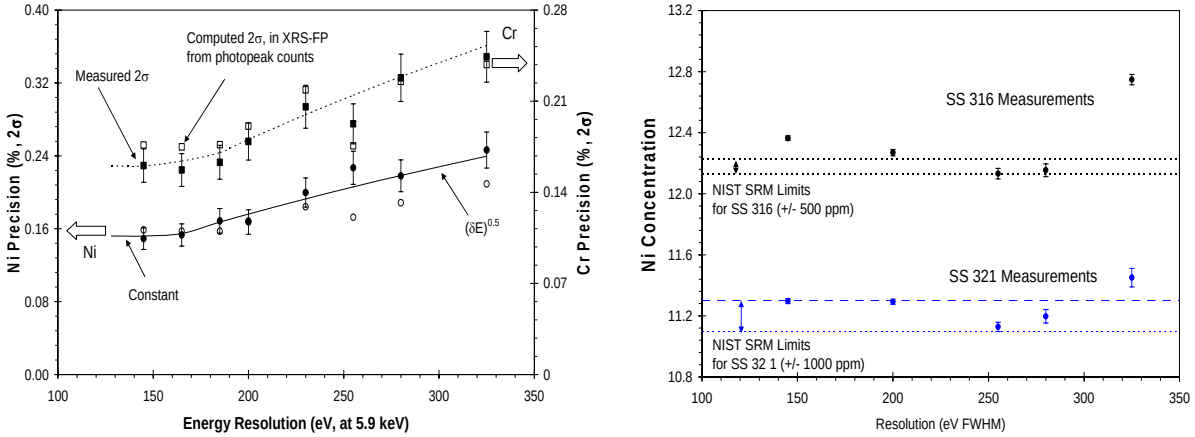

Figure 2. Left: Plot showing the precision of the analysis results for Cr and Ni in a stainless steel alloy as a function of energy resolution. Right: Plot showing the accuracy for Ni in steel.

The accuracy was measured using two NIST SRMs, SRM 1155 (SS 316) and SRM 1171 (SS 321). At each energy resolution, a 20 minute spectrum was obtained for SS 321 and used to calibrate FP, using the nominal composition from chemical analysis. Then 50, one minute measurements were obtained using both SRMs, and for each the mean and standard uncertainty of the mean were computed. The difference between this mean value and the composition from chemical analysis is the measured accuracy. Figure 2 (right) depicts the accuracy of the results for Ni. For SS 321, the sample used for calibration, the reported results are within the NIST confidence limits except for the poorest energy resolution. For SS 316, the average of the four results obtained below 300 eV is within measurement uncertainty of the chemical results. For neither sample is there a clear trend with energy resolution below 300 eV. Only at the poorest energy resolution was the accuracy significantly degraded and the results significantly worse than the confidence limits of chemical analysis. Similar results were obtained for Cr.

Figure 3 depicts the precision and accuracy of the analysis results for Mo, an isolated peak on some background. This plot shows that the precision is independent of energy resolution, as expected from Eq. [1]. The open circles in this plot show the random uncertainty computed by XRS-FP from photopeak counts alone, while the open square show the random uncertainty computed from photopeak and background counts. Accuracy exhibits no trend with energy resolution. The SS 321 results are in the confidence interval, while the SS 316 result averaged 200 ppm above the reference value (which has a 2σ confidence interval of +/-100 ppm).

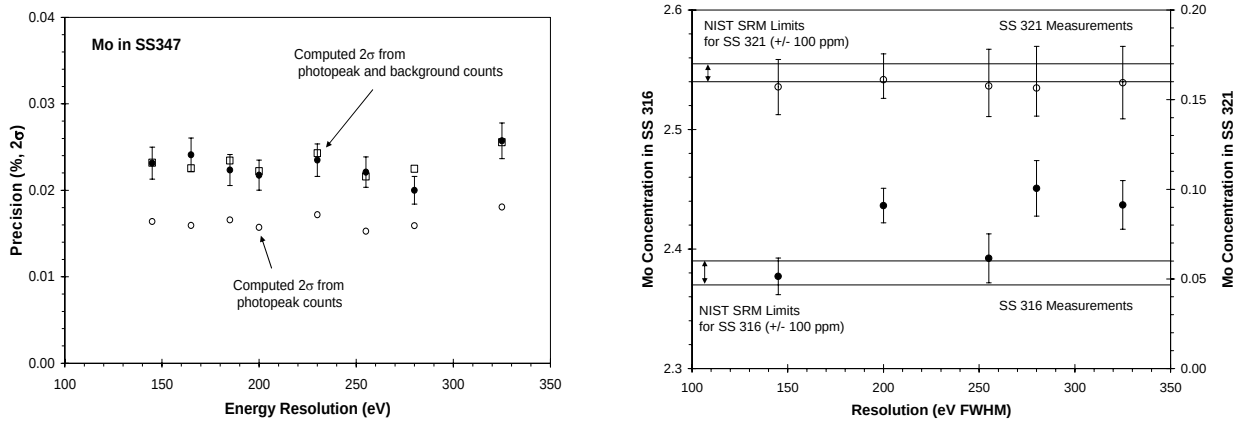

Figure 3. Plots showing the precision and accuracy of the analysis results for Mo in steel.

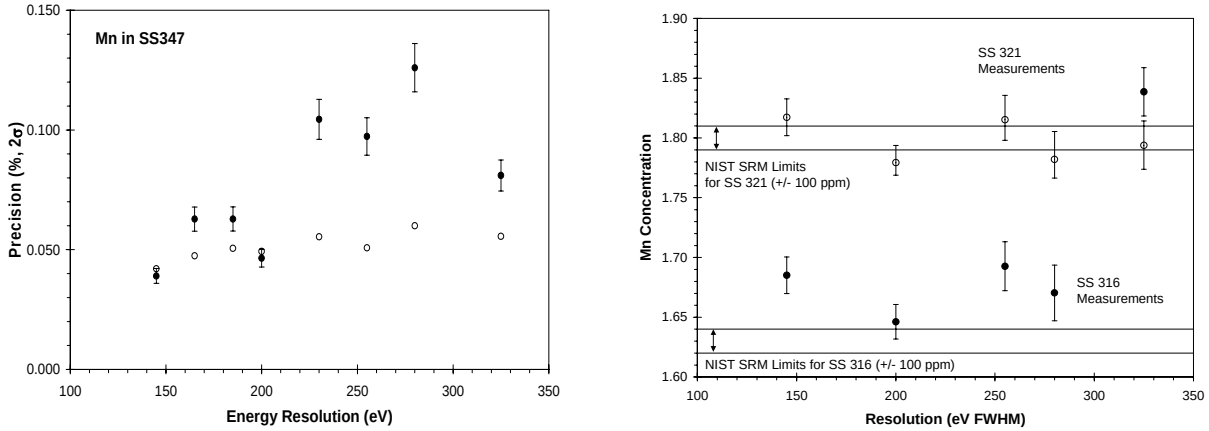

Figure 4. Plots showing the precision and accuracy for Mn in steel.

The Mn results, shown in Figure 4, depend much more strongly on energy resolution, exhibit significant scatter, and are larger than values computed from counting statistics. The scatter and large values imply terms other than counting statistics are important. For example, the corrected photopeak area for Mn depends quite strongly on spectrum processing parameters, such as terms used in background removal. This is a much stronger effect for Mn than for the more clearly defined peaks. Additionally, the nonlinear deconvolution algorithm can converge to local minima rather than the true minimum. Figure 4 illustrates the general trend of rapid degradation with energy resolution but also shows the importance of terms other than counting statistics. The accuracy of the Mn results exhibited no trend with energy resolution below 300 eV. For this range, the SS 321 measurement was within the confidence interval, while the SS 316 result averaged 150 ppm above the reference value (2σ confidence interval of +/-100 ppm). At the poorest energy resolution, the SS 316 result exhibited a systematic error of 0.2%.

In a real system, one would not intentionally degrade the resolution by operating at a higher temperature than necessary. Instead, one might change τ_p, since a short τ_p leads to degraded energy resolution but improved count rate capability. Figure 5 (left) shows precision as a function of τ_p for the SDD. The beam current was adjusted to maintain 10% dead time, with all data acquired for 60 sec. This plot shows that, for an SDD measuring steel, increasing count rate is more important than maximizing energy resolution, below 200 eV. Figure 5 shows similar

results with a 6 mm^2 Si-PIN. The resolution of the Si-PIN degrades much more rapidly than the SDD at short peaking times, leading to optimum performance at τ_p near 2 μsec.

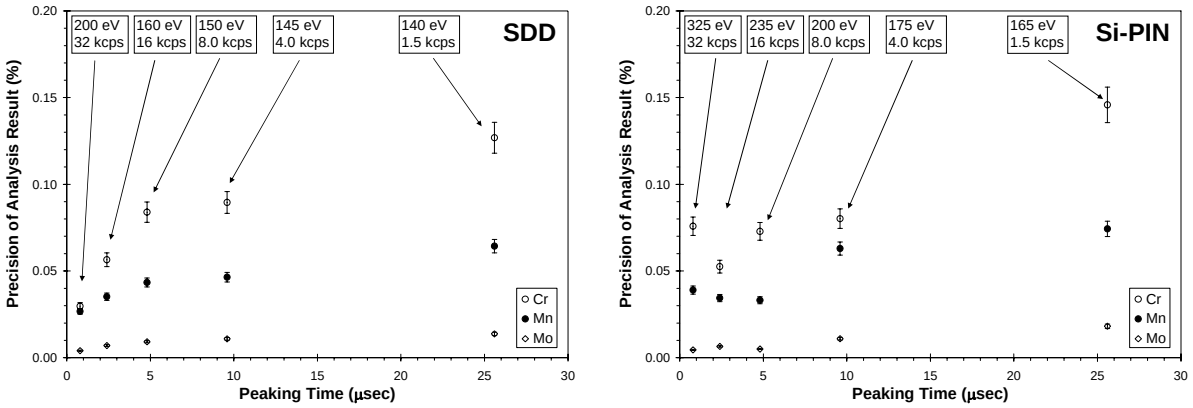

Figure 5. Plots showing the precision of the analysis result as a function of peaking time in the PX4 for the SDD (left) and a Si-PIN (right).

5. Experimental Results for Other Samples

How well do these results apply to other samples? The first additional sample studied, white gold, has a more complex spectrum than steel. White gold consists of approximately 75% Au. Some alloys use a Ni/Zn/Cu mixture, while others include Pd or Pt, and all may have a Rh plating. The analysis therefore included all of these elements: Ni, Zn, Cu, Pt, Pd, Rh, and Au, yielding many overlapping L lines to be analyzed.

Figure 6 (left) shows the spectrum measured from this sample (a wedding band). This particular sample obviously used the Ni/Zn/Cu composition. These lines are clearly seen, along with the L and M lines of Au. For this sample, 100 measurements were made at each of four energy resolutions. Standardless analysis was used since no appropriate calibration standard was available. Figure 6 (right) shows the precision of the results, exhibiting a very strong dependence on energy resolution. For this complex spectrum, some improvement of the measurement was obtained even at the lowest available energy resolution. This confirms Statham's result that energy resolution is most important for many overlapping peaks.

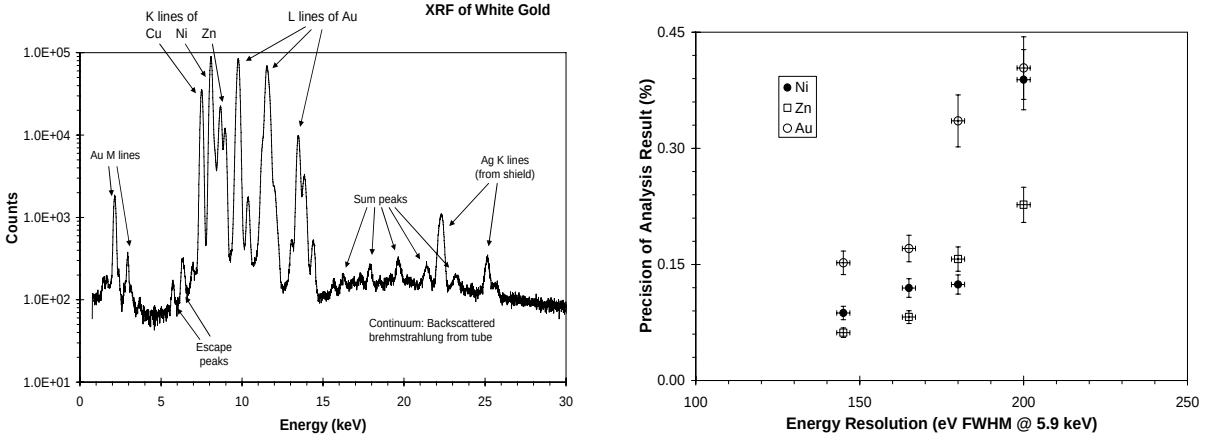

Figure 6. Left: Spectrum measured from a white gold ring. Right: Precision of analysis results for a complex spectrum, where the analysis included Ni, Zn, Cu, Pt, Pd, Rh, and Au.

The second additional sample studied, lead in paint on a wood substrate, represents a very simple spectrum. Lead paint applications typically require screening for lead concentrations greater than 1.0 mg/cm^2, with an uncertainty of 0.1 mg/cm^2. A calibration spectrum was measured using a 3.5 mg/cm^2 standard and then 100, 60 sec measurements were obtained at several energy resolutions. In all cases, precision was < 0.04 mg/cm^2, far exceeding the requirement. The precision exhibited no trend with energy resolution and, for many data points, was far larger than that predicted by counting statistics. The additional variability arose from fluctuations in the output flux of the X-ray tube, which were observed to be about 0.5%. The steel and white gold analyses determined ratios of elemental concentrations, which are independent of absolute beam flux. Lead paint analysis depends on the absolute flux, and with sufficient counts, beam flux variability dominated, so energy resolution did not matter.

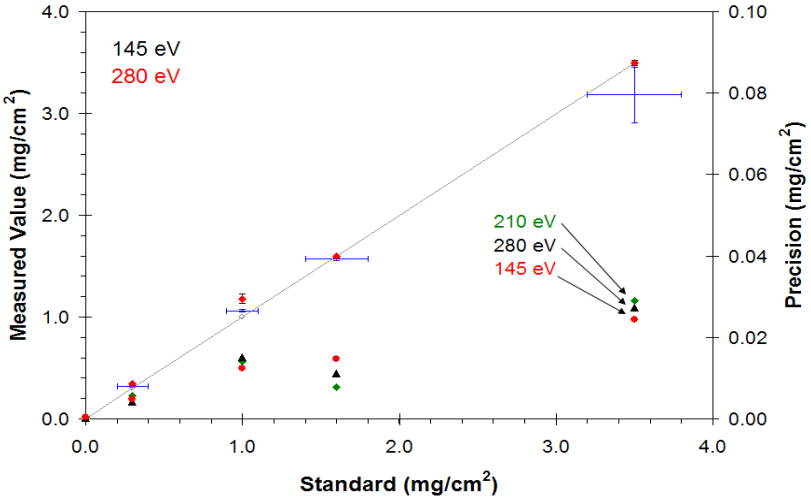

Figure 11. Plot showing the results of lead paint measurements at different energy resolutions.

For the third additional case, the performance of the SDD system was compared with a CdTe based system for measuring the composition of a Pb-Sn solder (NIST SRM 1131). The CdTe detector has an area of 25 mm^2, four times the area of the SDD. It has a thickness of 0.75 mm, and combined with its higher Z, it has a far higher sensitivity. At the energies of the Pb K lines, where there are negligible environmental interferences, sensitivity is >80% [6]. On the other hand, it has poorer energy resolution, 450 eV FWHM at 5.9 keV. A ^{57}Co isotopic source was the excitation source for CdTe. To normalize for counting statistics, data were taken using the same source fluence. The flux was measured from the X-ray tube, at 40 kVp and 15 μA with an Al filter, at 30 cm distance, and then at the same distance from the isotopic source. The CdTe measurement time was increased to obtain the same equal fluence. The SDD data were taken at two energy resolutions, 145 and 325 eV FWHM (measured at the 5.9 keV Mn line).

	Sn Conc.	Pb Conc.
SDD (145 eV FWHM)	39.226 ± 0.240	60.342 ± 0.240
SDD (325 eV FWHM)	39.174 ± 0.334	60.364 ± 0.327
CdTe (450 eV FWHM)	39.624 ± 0.305	60.376 ± 0.304

Table 1. Results of 60-40 Pb-Sn solder analysis using an SDD and a CdTe detector.

Table 1 shows that the precision of the CdTe was better than that of the SDD at 325 eV, though worse than the SDD at its optimum. This measurement was carried out on a sample of pure solder, with only Sn and Pb. If one measures solder on a printed wiring board, then many additional elements will generally be present, such as Cu, Br, Cr, Ti, etc. These elements interfere with the Pb L lines but not the K lines, degrading the SDD results but not the CdTe results.

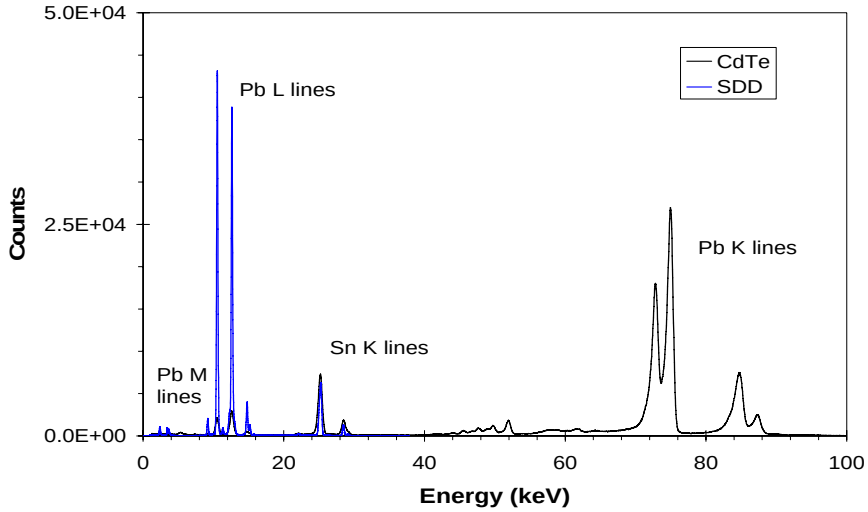

Figure 12. Spectra measured for a 60-40 Pb-Sn solder, using (1) a silicon drift diode and a 40 kVp X-ray tube and (2) a CdTe detector and a ^{57}Co isotopic source. The CdTe detector has much higher sensitivity, particularly at the energies of the Pb K lines where there are few interferences, but has much lower energy resolution.

6. Conclusions

The data confirm that, for major peaks with some overlap and background, such as Cr and Ni in steel, the precision is independent of resolution for the highest resolutions, then begins to degrade with a $(\delta E)^{0.5}$ dependence. For a small peak with much overlap, such as Mn in steel or Au in white gold, the precision degrades rapidly with energy resolution. For isolated peaks not dominated by background, such as Mo in steel, the precision is independent of energy resolution. The accuracy of the analysis results was shown to be independent of resolution, except for the very worst resolution studied here.

The data showed that terms other than counting statistics can dominate precision. This was clearly seen for Mn in steel, in which the precision was presumably dominated by the details of the spectrum processing parameters and deconvolution algorithm, and for Pb in paint, in which the variations in beam intensity dominated precision.

For steel alloys in this system, little benefit is found if the resolution is reduced below 200 eV. A much better analysis is obtained by increasing counting statistics while keeping resolution at 200 eV. For the SDD, short peaking times with maximum beam intensity provided the best results. For the Si-PIN, the optimum occurred at a resolution near 200 eV FWHM.

The benefit of improved resolution depends on the detector, on the sample, and on the goals of the analysis. For relatively simple spectra with widely spaced peaks, counting statistics matter

more than resolution. The optimum system uses a high sensitivity detector and maximum count rate. For complex spectra with overlapping peaks, analysis of L lines, and the presence of trace elements, energy resolution is very important. Resolution should be improved to the point where the peaks become separated, beyond which improving counting statistics will improve precision.

7. References

[1] P.J. Statham, *Quantifying benefits of resolution and count rate in EDX microanalysis*, Chap 8 in X-ray spectrometry in electron beam instruments, ed. D. Williams, J. Goldstein, D. Newbury, Plenum Press, pp 101-126 (1995).

[2] T. Arai, *Analytical precision and accuracy in X-ray fluorescence analysis*, The Rigaku Journal, Vol 21, No. 2, pp 26-30, (2004).

[3] P. Bevington, K. Robinson, **Data Reduction and error analysis for the physical sciences**, 2nd edition, McGraw-Hill, Boston MA, (1992), p 2.

[4] Redus, R.H., J. Pantazis, A. Huber, T.Pantazis, *Improved sensitivity X-ray detectors for field applications*, IEEE Trans. Nucl. Sci. Vol. 49, No. 6, p.3247, Dec 2002.

[5] Redus, R.H., A. Huber, J. Pantazis, T.Pantazis, D. Sperry, *Design and performance of the X-123 compact X-ray and gamma-ray spectroscopy system*, 2006 IEEE Nuclear Science Symposium Conference Record. R15-4.

[6] Redus, R.H, J. Pantazis, T. Pantazis, A. Huber, B. Cross, *Characterization of CdTe detectors for quantitative X-ray spectroscopy*, in press, IEEE. Trans. Nucl. Sci.